Quantification of rut depth in geogrid reinforced asphalt overlays using accelerated pavement testing

N. S. Correia
University of Sao Paulo, Sao Carlos, Brazil
J. G. Zornberg
The University of Texas at Austin, Austin, Texas

Correia, N.S., and Zornberg, J.G. (2014). "Quantification of Rut Depth in Geogrid Reinforced Asphalt Overlays using Accelerated Pavement Testing." Proceedings of the *10th International Conference on Geosynthetics*, 10ICG, Berlin, Germany, 21-25 September 2014 (CD-ROM).

ABSTRACT: Rutting results from permanent vertical deformation in one or more layers of an asphalt pavement, which severely impacts the pavement serviceability and durability. Geogrid reinforcement within the asphalt layer of a flexible pavement can facilitate load distribution and reduce rutting depth due to the resulting increase of the pavement overall stiffness. However, only limited research has been conducted on the impact of geosynthetic reinforcements in asphalt overlays to reduce asphalt surface plastic deformation. This work aims at studying the benefits of polymeric geogrid reinforcement within asphalt overlays using tests results generated in an accelerated pavement testing facility. Full-scale asphalt pavement models were constructed in the laboratory and loaded using a rolling wheel simulating the load of a truck wheel. Instrumentation allowed measurements of the rutting profiles as a function of the number of wheel passes, as well as the monitoring of dynamic vertical stresses at the bottom of the asphalt layer and a top of the subgrade. The results of a reinforced pavement section were compared to those of an unreinforced section. The permanent deformation response has clearly shown an improved performance when using geogrid asphalt reinforcement. The reinforcement mechanism could be quantified by the reduction in rutting and reduction of the vertical stresses in pavement layers.

Keywords: reinforcement; polymeric geogrid; asphalt overlay; rutting; accelerated pavement testing.

1 INTRODUCTION

Rutting results from permanent vertical deformation in one or more layers of an asphalt pavement, which severely impacts the pavement serviceability and durability. Besides pavement structural damage, surface rutting poses serious safety threats to drivers due to the depression in the pavement surface along the wheel path. Some measures have been adopted to mitigate rutting in asphalt pavement such as using modified asphalt binder, innovating aggregate gradation, and adding fibers or geosynthetic reinforcements to the asphalt layer.

Previous research into geogrid reinforcing asphalt concrete layers has focused primarily the prevention of reflection cracking. This included the use of fatigue asphalt beams tests (Brown and Brodrick, 1985; Austin and Gilchrist 1996; Brown et al., 2001, Montestruque et al. 2004; Khodaii et al., 2009), as well as accelerated trafficking devices or field studies (Ling and Liu 2001, Sobhan and Tandon 2003; Gallego and Prieto 2006, Chehab and Tang 2012; Yu et al. 2013). However, only limited research have been conducted on the impact of geogrid as a structural reinforcement inclusion within asphalt overlays to reduce rutting in asphalt pavements. Geosynthetic reinforcement systems can be employed in new asphalt layers or during repairs by improving the mechanical properties of the pavement to resist cumulative displacements (Austin and Gilchrist 1996; Wasage et al. 2004; Laurinavičius and Oginskas, 2006; Solaimanian; 2013), as well as lower vertical subgrade stresses (Siriwardane et al., 2010) by the increase of stiffness in the asphalt layer.

Reducing time and inconvenience to motorists by building more reliable, longer lasting and less expensive maintenance roads is an important issue when considering the cost-effectiveness of pavements. Furthermore, asphalt resurfacing designs usually do not consider the geosynthetic in the asphalt layer due to a

lack of understanding of the governing mechanisms of the geosynthetic, especially regarding quantifying the reinforcement benefits.

A reliable method for quantifying the effectiveness of geosynthetic technology in pavements is by testing full-scale pavement sections and measuring the pavement response to traffic loading using field instrumentation. Pavement instrumentation has become an important tool in monitoring pavement performance and quantitatively measuring pavement system responses such as strain, stress and deflections under traffic loading conditions. Accelerated pavement testing has become an effective intermediate between testing of real field pavement sections and laboratory tests, particularly by shortening the period of road deterioration into just few weeks of testing.

The aim of this work is to study the benefits of geogrid reinforcement within asphalt overlays to reduce pavement rutting using tests results generated in an accelerated pavement testing facility. Full-scale asphalt pavement models were constructed in the laboratory and loaded using a rolling wheel simulating the load of a truck wheel. The results of reinforced pavement sections are compared against those of an unreinforced section.

2 TESTING PROGRAMME

2.1 *Wheel tracking apparatus*

Full-scale asphalt pavement models were constructed in the laboratory and loaded using a rolling wheel simulating the load of a truck wheel. The wheel tracking apparatus was installed in a large steel test box with internal dimensions of 1.8 m (length), 1.6 m (width) and 1.80 m (length). The test box was designed with steel reinforced walls to withstand high lateral soil stresses with minimum resulting lateral deformations, thereby achieving plane strain state in the structure. The stiffness of the structure was enhanced by a reaction beam, fixed on the walls of the box, which completes the load transfer system. To accurately represent the structural sections of the asphalt pavement, the testing box was filled with three pavement materials: subgrade soil, aggregate granular base and hot mix asphalt wearing surface.

The wheel load is controlled by a hydraulic jack designed to apply a load of up to 2 tons, while a hydraulic motor controls the movement of the system (wheel + jack + load cell). Wheel speeds up to 25 passes per minute can be achieved. The tracking apparatus has an in-built counter that registers the number of wheel passes. The useful testing length of the moving wheel (at constant speed) covers a distance of 1.0 m. The wheel involves a rubber tire mounted on a steel wheel of 546 mm diameter by 154 mm wide. The tire inflate pressure was set to 700 kPa. Figure 1a illustrates the wheel tracking apparatus.

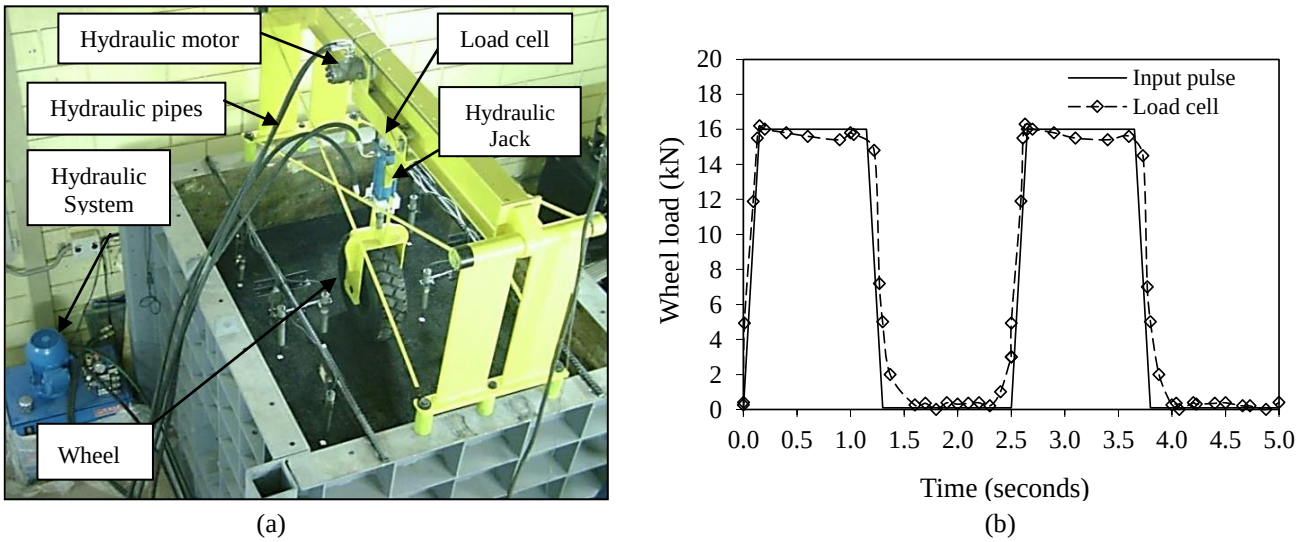

(a) (b)

Figure 1. Pavement Testing Facility: (a) wheel tracking device; (b) wheel load pulse and corresponding load cell measurement.

An in-house software programme for data acquisition was developed to control the load-time history applied to the wheel (cyclic moving wheel load mode). The same data acquisition was used to collect data from the instruments installed in the pavement sections. The software was programmed to induce the load and wheel pressure pulse shown in Figure 1b. The wheel load pulse has a linear load increase from 0 to 16 kN over a 0.1 second rise time, followed by 1.0 second period when the load is held constant, then a load

decrease to zero over a 0.1 second period and finally a 1.2 second period load before the load cycle is repeated, resulting in a load pulse frequency of 2.4 Hz. Also shown in Figure 1b, is the corresponding output from the load cell for a typical load application, showing a very good correlation between the target and actual measured loads. The tire contact pressure of 700 kPa was used for the tests, achieved with an applied load of 16 kN.

2.2 *Pavement materials and layer properties*

The different materials used in the test sections include hot mix asphalt concrete, base aggregate and subgrade soil. The soil described as SP-215 (from station 152 + 600 km at Sao Carlos – Sao Paulo) was chosen for the artificial subgrade. The soil is classified as MH and A-7-5 according to the Unified Soil Classification System and AASHTO classification system, respectively. California Bearing Ratio (CBR), bulk density and the moisture content were measured for each 250 mm thick layer. The average maximum dry density and optimum moisture content of the soil were 15.0 kN/m^3 and 29%, respectively. The CBR was 4.5 %, which represents a relatively weak subgrade condition. The subgrade was prepared in the test box in lifts of 50 mm thick, by drop hammer manual compaction. The total subgrade thickness was 1.0 m.

The aggregate material is classified as GP and A-1-a according to the Unified Soil Classification System and the AASHTO classification system, respectively. The aggregate is a non-plastic (NP) 100% passing no. 1 opening sieve and 6% passing no. 200 opening sieve. The uniformity coefficient (Cu) was 46.85 and a coefficient of curvature (Cc) was 4.8. The maximum dry density is 24 kN/m^3 and the optimum moisture content is 6.5% in relation to standard Proctor tests. Base layer compaction was carried out in lifts of 100 mm thickness (total base thickness of 200 mm) with a vibratory plate and average degree of compaction of 99.5%.

Hot mix asphalt concrete (HMA) material was obtained from a local plant. The HMA is a 9.5 mm (3/8") dense-fine-graded mixture with an asphalt binder content of 5.4%, indicated for all traffic conditions (FHWA & NAPA Information Series 128, 2001). The HMA layer was compacted with vibratory plate over the base course in one lift of 50 mm.

Both unreinforced and geogrid-reinforced pavement sections were constructed for testing in two series. The first stage of tests were performed at a time corresponding to immediately after the first 50 mm of asphalt concrete was placed (Control sections). The second series of tests (Resurfaced sections) were performed after the Control sections had been first loaded by simulated traffic. For the second stage of tests, an asphalt overly of 60 mm was placed over the previously degraded asphalt layer. Figure 2 shows the flow chart of the test procedure for both first and second stages of tests. The resurfaced sections included one test with a geogrid as reinforcement and another without reinforcement.

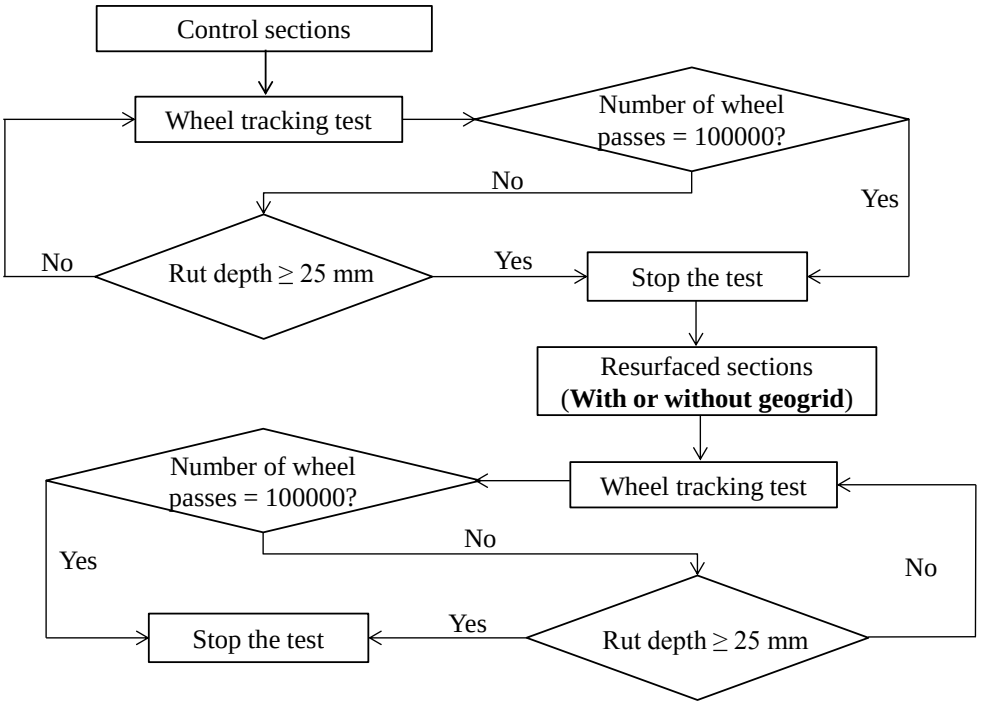

Figure 2. Flow chart of APT tests using wheel tracking machine for unreinforced and geogrid reinforced sections.

HMA theoretical maximum density (TMD) values of 2.676 and 2.677 were obtained for unreinforced and geogrid reinforced tests, respectively. The air void contents of the asphalt surface courses for unreinforced sections were 9.84% (first stage) and 10.20% (second stage). For the geogrid reinforced section, the air void contents of the asphalt surface courses were 13.42% (first stage) and 14.41% (second stage).

2.3 *Geogrid characteristics and installation process*

A geogrid composite specifically designed for asphalt reinforcement was selected for the reinforced pavement section. The geogrid manufactured from high-modulus poly-vinyl alcohol (PVA) is oriented in two directions, forming a biaxial product with quadrangular apertures. An ultra-lightweight polypropylene (PP) nonwoven geotextile is attached on one side of the geogrid to facilitate the installation and to allow a continuous bonding. The material is pre-coated with bitumen in order to promote a better adherence with the asphalt layers. Index tests were conducted and the results are presented in Table 1.

Table 1 - Specifications of the geosynthetic used in this research.

Properties	**Characteristics**		**Geogrid**	
Mechanical properties of the geogrid	Tensile strength (kN/m) ASTM 6637 (2011)	at 2% of strain	MD	13.32
			CMD	17.72
		at 5% of strain	MD	36.28
			CMD	41.89
		Ultimate	MD	40.51
			CMD	46.91
Physical properties of the geogrid	Aperture dimension (mm)		MD	40.00
			CMD	40.00
	Mass per Unit area (g/m^2)		240.0	
	Polymer of the geogrid		poly-vinyl alcohol	

MD = Machine direction; CMD = Cross Machine direction.

After the first stage of tests, the geogrid was cut into the dimensions of the box area and then placed flat over the asphalt layer with geotextile fabric facing down. The machine direction was parallel to wheel tracking path. Previous to the geogrid installation, a tack coat rate of asphalt emulsion of 0.6 l/m² was sprayed over the previously tested HMA layers, according to DNER-SP ET-DE-P00/043 (2006). The asphalt overlay was then compacted directly over the geogrid. For the unreinforced test section, the same tack coat rate was used. Figure 3 illustrates the geogrid used in this research and the installation over the underlying asphalt layer.

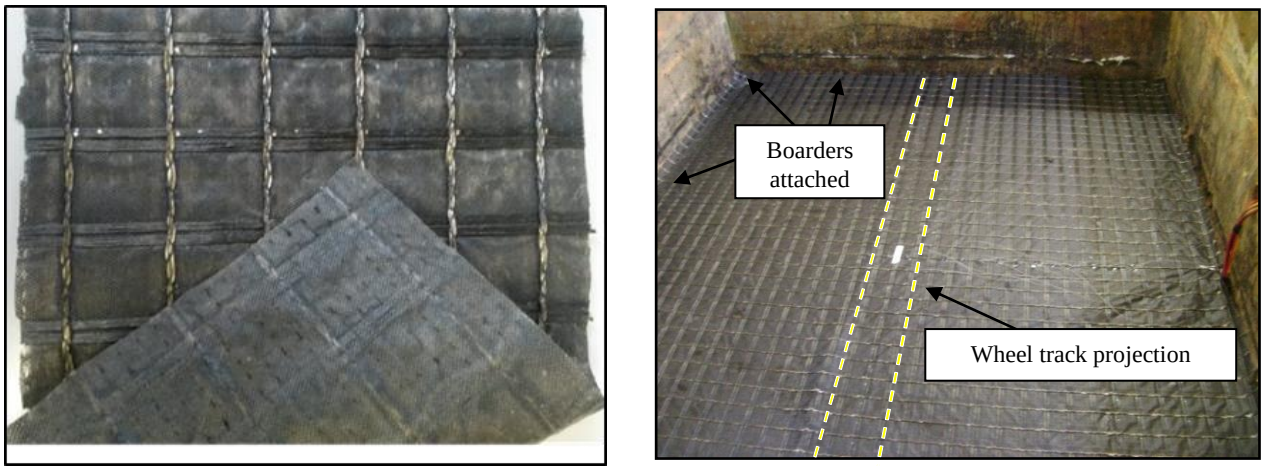

(a) (b)

Figure 3. Geosynthetic reinforcement: (a) geogrid composite; (b) view of the geogrid after installation.

2.4 *Instrumentation*

Instrumentation was installed to measure pavement stresses and deformation in the test sections in order to quantify the mechanical response of the pavement materials. Data acquisition software was configured to record information on the full time-history of response for described load cycles. A total of eight linear variable differential transformers (LVDT) were used to monitor surface deformation of the asphalt concrete layer, with ranges of 50 and 100 m. The LVDTs allowed measurements of the plastic deflection as a function of the number of loading wheel passes. Soil stress cells were placed in both base course and the subgrade in order to quantify the dynamic stress behaviour of the system. Figure 4 illustrates the pavement sections layout, sensor location and rutting measurement procedure.

Additional permanent deflection profiles were measured by using a perfilometer (Figure 4b) in the vicinity of the load at 1, 10, 100, 500, 1000, 2500, 5000 passes, and then at intervals of 10000 wheel passes. The surface profile for the analyzed cross section was determined by first taking profile measurements before pavement loading (pass level 0), where the reference was taken. The asphalt surface course was painted white to better visualize markers and cracks development.

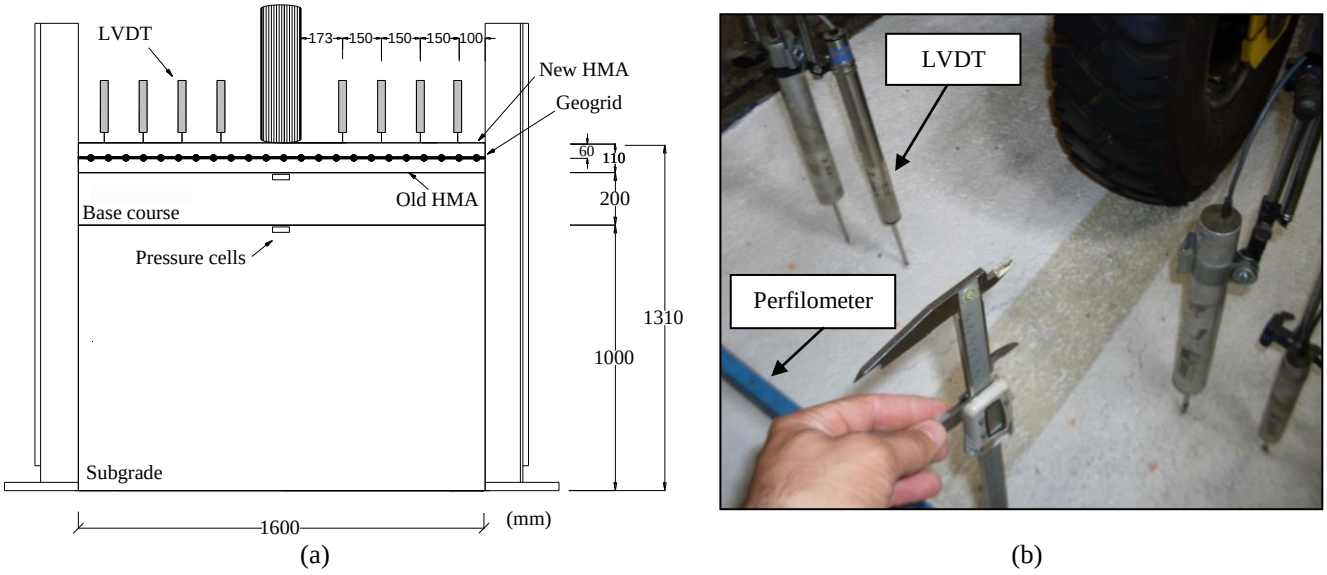

Figure 4. Instrumentation: (a) pavement sections layout and sensor location; (b) rutting measurement procedure.

3 RESULTS

3.1 *Rutting quantification*

The development of permanent deformations (rutting) on the pavement surface due to permanent vertical strains in pavement layers was measured for both reinforced and unreinforced tests. Measurements were conducted according to the flow chart shown in Figure 2. Control sections C1 and C2 correspond respectively to the first stage of tests for unreinforced and geogrid reinforced tests. The rutting behaviour for the first stage of tests C1 and C2, and second stage (unreinforced and geogrid reinforced tests) are shown in Figure 5. A comparison of rutting between test sections has been conducted in two ways. First, the maximum rut a depth along the wheel path was averaged for each pass level as a function of the number of wheel passes (Figure 5a). Figure 5b shows the rutting plotted as a function of the number of wheel load at the end of the test (N=100000). The results from Control sections C1 and C2 have indicated excellent repeatability of overall rutting behavior and sensors response for two identical test sections, providing confidence in using the quality control measures. No significant asphalt fatigue problems were noted in control test sections.

The results are suitable to compare the performance of the various sections in terms of rutting for unreinforced and geogrid reinforced sections. The traffic benefit ratio (TBR) is defined as the number of cycles to reach a particular permanent surface deformation, for a reinforced test section, divided by the number of cycles to reach this same deformation in an unreinforced test section. Based on average rutting measurements, a TBR value of 4.33 corresponding to a rut level of 3 mm was obtained comparing reinforced section with unreinforced section. TBR results have indicated more than quadruplicating increase in

pavement's life improvement when using geogrid asphalt reinforcement. For the reinforced test section, significant TBR values were also measured for the initial millimeters of permanent deformation, indicating that benefits due to reinforcement were realized immediately upon load application. Deformations corresponding to this test stage were seen in all pavement sections and were reduced by the presence of reinforcement. The results obtained in this research with a polymeric geogrid are consistent with results obtained from some field monitoring programs. In a research conducted by Siriwardane et al. (2010), the cumulative displacements have decreased with the inclusion of a fiber glass geogrid within the asphalt layer with an improvement of approximately 40%. In a study conducted by Perkins (1999), results show that placing a geogrid at a certain depth in the base layer had provided superior rutting performance than placing the same geogrid at the base-subgrade interface, suggesting that moving the geogrid closer to the surface would provide better performance.

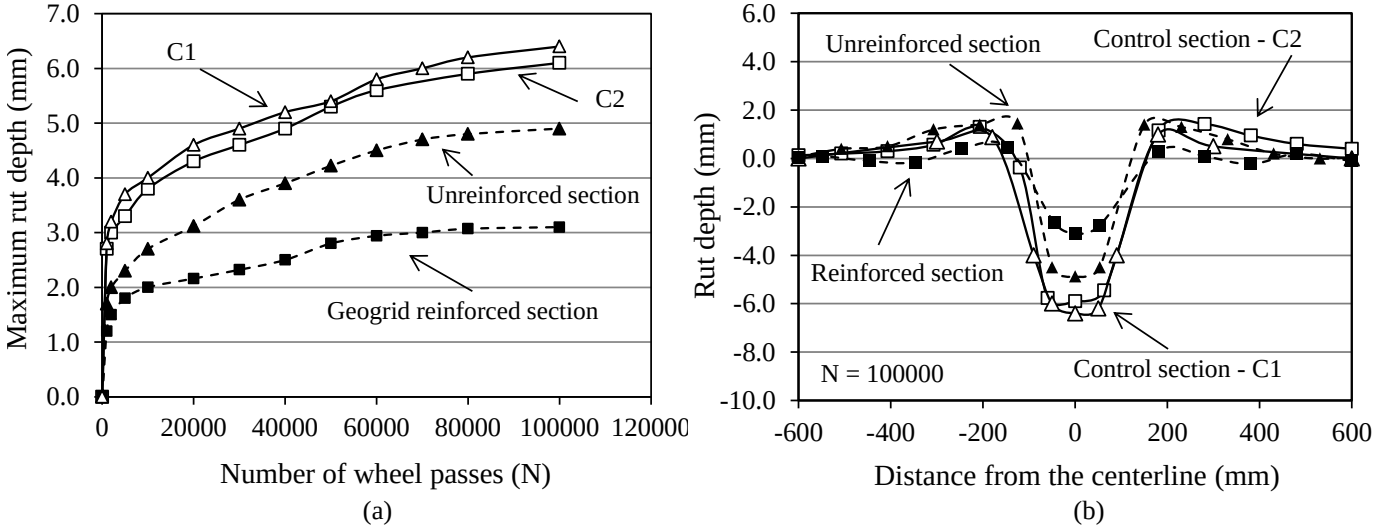

Figure 5. Rut depth results: (a) maximum results along the wheel path; (b) rut profile at N=100000.

Additionally, the unreinforced case shows significant heaving next to the loading area when compared to the geogrid reinforced test (Figure 5b), both with similar asphalt surface course volume of air voids. These results suggest that the geogrid reinforcement placed at the bottom of the HMA overlay effectively reduced shear deformation and heaving of the asphalt surface course. When the load is applied to the surface of the pavement, a zone of tension is developed at the lower section of the asphalt concrete layer. The tensile stress acts in the asphalt concrete and is transferred to the geogrid as tensile force.

Figure 6 illustrates Relative vertical displacements results plotted as the measured relative vertical displacements versus the number of wheel passes. This analysis was conducted after the first 10000 load cycles since an excessive deformation due to the high air void contents of the asphalt surface was observed for all test sections. Comparing the second series of tests (Resurfaced sections), results indicate that there was a fundamental difference between geogrid reinforced and unreinforced cases, enhancing pavement lifetime.

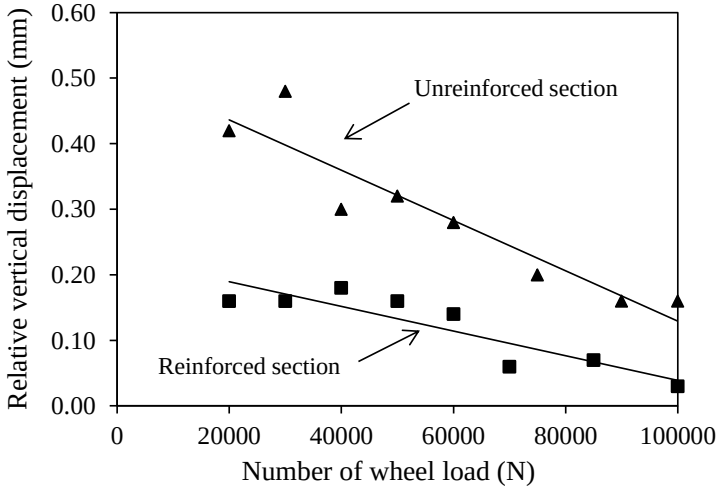

Figure 6. Relative vertical displacements versus number of wheel passes.

3.2 *Dynamic stress response*

Instrumentation have also allowed the evaluation of stresses induced during loading wheel passes (dynamic stress response of the test sections). Instrumentation from the stress cells located at the bottom of the asphalt layer and at the top of the subgrade layers were examined (Figure 4a) beneath the wheel path. The typical dynamic response for a given time during the test is shown in Figure 7 for both unreinforced and geogrid reinforced test sections.

Stress response measures from APT tests sections have shown a marked difference between reinforced and unreinforced sections, both at the bottom of the HMA layer (Figure 7a) and at the top pf the subgrade (Figure 7b). These results are consistent with those reported by Perkins (2002), although testing a geogrid reinforcing the aggregate base layer of a flexible pavement. In the research conducted by Siriwardane et al. (2010) with the inclusion of a fiber glass geogrid within the asphalt layer, it was concluded that the geogrid reinforcement have spread the circular load over a larger area in the lower layers of the pavement section causing lower vertical subgrade stresses.

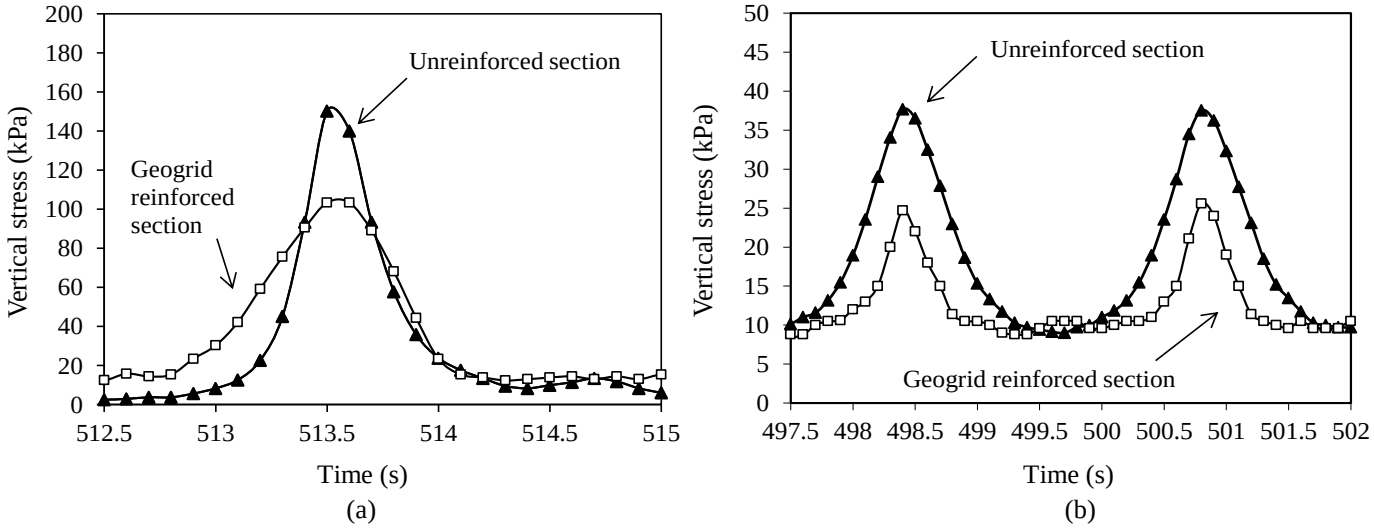

Figure 7: Typical vertical stress dynamic response: (a) at the bottom of old HMA; (b) at the top of the subgrade.

Figure 8 shows the time-history of dynamic stress throughout tests. An average of 32% reduction in dynamic vertical stress at the bottom of the asphalt layer was observed in the geogrid reinforced section in relation to unreinforced section (Figure 8a). Figure 8b shows that the dynamic vertical stresses induced in the top of the subgrade are 36% reduced by the presence of reinforcement in the asphalt layer. The results show that pavement layer stress measurements can be made with a very high degree of repeatability and reliability. The standard deviations of the results ranged from 0.90 to 5.46 kPa and coefficient of variation ranged from 2.35 to 3.69 percent.

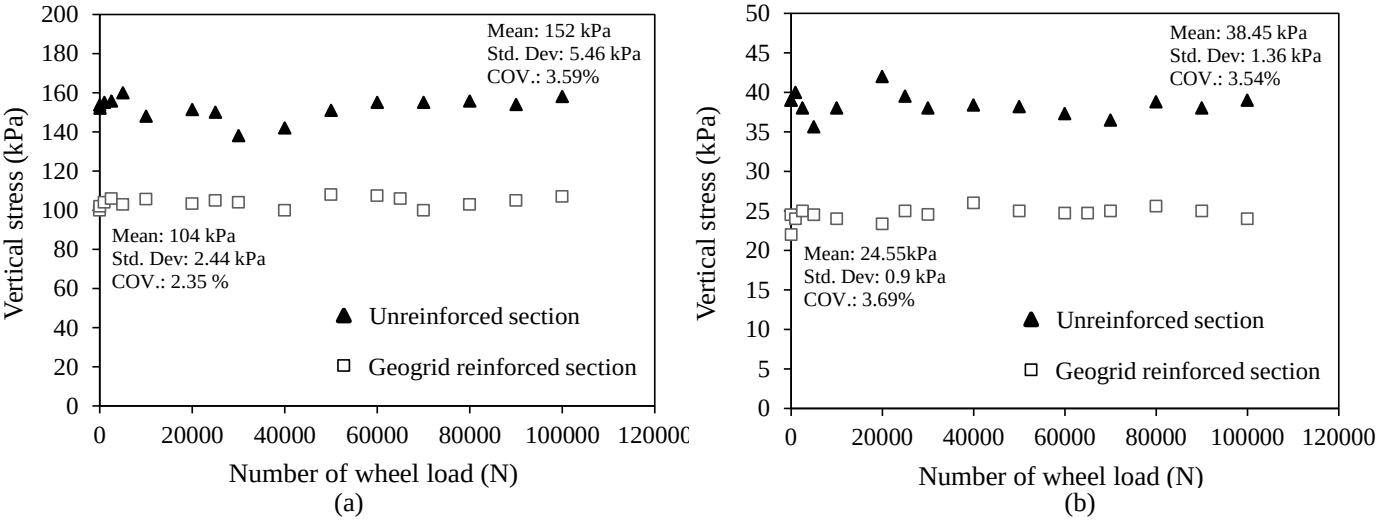

Figure 8: Dynamic stress response as function of wheel passes: (a) at the bottom of HMA; (b) at the top of the subgrade.

4 CONCLUSIONS

The objective of this work was to quantify the benefits of geogrid reinforcement within asphalt overlays to decrease pavement rutting using results generated in an accelerated pavement testing facility. The results of reinforced pavement sections were compared to those of unreinforced sections. Based on the results obtained from this research, the following conclusions can be made:

1. Based on rutting measurements, the service life of a geogrid reinforced asphalt layer was found to be over four times longer than that of an unreinforced asphalt layers. The results shows the polymeric geogrid reinforcement have effectively reduced shear deformation and heaving of the asphalt surface course.

2. Measures from APT test sections showed a significant difference in the stresses measured over the subgrade between the geogrid reinforced and unreinforced sections. Specifically, an average reduction of 32% in dynamic vertical stress at the bottom of the asphalt layer was observed when using geogrid reinforcement. In terms of reduction in dynamic vertical stress at the top of the subgrade, an average of 36% was obtained.

The reinforcement mechanism of PVA geogrid within the asphalt layer could be quantified by instrumentation placed in the test sections. These mechanisms include a reduction in permanent vertical deformation (rutting) and greater reduction of the vertical stresses in pavement layers.

ACKNOWLEDGMENTS

The authors gratefully recognize Professor Benedito de Souza Bueno contributions to this study, Huesker for the technical, guidance and financial support and CNPq for the research fellowship.

REFERENCES

ASTM D 6637. 2011. Standard Test Method for Determining Tensile Properties of Geogrids by the Single or Multi-Rib Tensile Method, Oct 1, 2011.

Austin, R. A. & Gilchrist, A. J. T. 1996. Enhance performance of asphalt pavements using geocomposites. Geotextiles and Geomembranes, 14, p. 175-186.

Brown, S. F. & Brodrick, D. A. B. 1985. Polymer grid reinforcement. Thomas Telford Limited. London, p. 158-165.

Brown, S. F., Thom, N. H., & Sanders, P. J. 2001. A study of grid reinforced asphalt to combat reflection cracking. Asphalt Paving Technology, 70, p. 543-571.

Chehab, G. R., & Tang, X. 2012. The use of a multi-set-up, reduced-scale accelerated trafficking simulator for evaluating roadway systems and products. International Journal of Pavement Engineering, 13, p. 535-552.

DNER-SP ET-DE-P00/043. 2006. Anti-reflective cracking systems with geosynthetics. Department of Highway of Sao Paulo State – Sao Paulo. Technical Specification, Sao Paulo, Brazil (*in portuguese*).

FHWA & NAPA (2001). HMA Pavement Mix Type Selection Guide. Information series 128. Federal Highway Administration, U.S. Department of Transportation. National Asphalt Pavement Association.

Gallego, J. & Prieto J. N. 2006. New laboratory equipment for study of reflective cracking in asphalt overlays. Transportation Research Record: Journal of the Transportation Research Board, No. 1970, Transportation Research Board, p. 215-222.

Khodaii, A., Fallah, S., & Moghadas Nejad, F. 2009. Effects of geosynthetics on reduction of reflection cracking in asphalt overlays. Geotextiles and Geomembranes, 27, p. 187-195.

Laurinavičius, A. & Oginskas, R. 2006. Experimental research on the development of rutting in asphalt concrete pavements reinforced with geosynthetic materials, Journal of Civil Engineering and Management, 12, p. 311-317.

Ling H. I. & Liu, Z. 2001. Performance of geosynthetic-reinforced asphalt pavements. Journal of Geotechnical and Geoenvironmental Engineering, 127, No. 2, p. 177-184.

Montestruque, G.; Rodrigues R.; Nods M. & Elsing A. Stop of reflective crack propagation with the use of PET geogrid as asphalt overlay reinforcement. Fifth RILEM International Conference Cracking in Pavement, Mitigation, Risk Assessment and Prevention. Limoges, France, pp. 231-238, 2004.

Perkins, S.W., 1999. Mechanical Response of Geosynthetic-Reinforced Flexible Pavements. Geosynthetics International, 6, No. 5, pp. 347-382.

Perkins, S. W. 2002. Evaluation of geosynthetic reinforced flexible pavement systems using two pavement test facilities. FHWA/MT-02-008/20040, 136p.

Siriwardane, H., Gondle, R., & Bora K. 2010. Analysis of Flexible Pavements Reinforced with Geogrids. Geotechnical and Geological Engineering, 28, p. 287-297.

Sobhan K. & Tandon V. 2003. Mitigating Reflection Cracking in AC Overlays over PCC Joints Using Geosynthetics. Final Report, Contract No. FHWA DTFH61-00-X-00098, Federal Highway Administration, Washington, D.C.

Solaimanian, M. 2013. Evaluating Resistance of Hot Mix Asphalt to Reflective Crackin Using Geocomposites. Report No. PSU-2008-04. The Mid-Atlantic Universities Transportation Center, Springfield, VA, 36p.

Wasage, T. L. J.; Ong, G. P.; Fwa T. F. & Tan, S. A. 2004. Laboratory evaluation of rutting resistance of geosynthetics reinforced asphalt pavement. Journal of the Institution of Engineers, Singapore. Vol. 44 Issue 2 2004, pp. 29-44

Yu, B., Lu, Q. & Yang, J. 2013. Evaluation of anti-reflective cracking measures by laboratory test, International Journal of Pavement Engineering, 14, p. 553-560